Instability of Spiral Viscous Flow in Annulus with Rotating and Moving Inner Cylinder

A. Nouri-Borujerdi[1], A. Kebriaee[2]

[1]School of Mechanical Engineering, Sharif University of Technology
[2]Department of Aerospace Engineering, Sharif University of Technology
([1]anouri@sharif.edu, [2]kebriae@sharif.edu)

Abstract- Instability of a viscous incompressible flow between two rotating concentric cylinders has been investigated by spectral method. The outer cylinder is stationary and the inner one rotates and moves axially simultaneously. Chebyshev tau method is used to solve eigenvalues of the flow stability. These eigenfunctions of governing equations are expressed by the Chebyshev polynomials. The method is a new approach to solve instability equation of the spiral Couette flow with execution time less than the other methods. Critical flow characteristics are calculated at the threshold of the instability for various Reynolds numbers based on the axial velocity. It is found that the axial velocity increases the flow stability and also non-symmetric mode is more stable than the symmetric mode for all Reynolds numbers. In addition, the velocity eigenmodes with more zero velocity points are attributed to the more stable conditions.

Keywords- instability, Taylor-Couette flow, Chebyshev tau method, numerical method

I. INTRODUCTION

A viscous flow between two concentric circular cylinders is called Taylor–Couette flow if one of the cylinders is stationary and the other one is rotating. The important of this study is elucidated in different industrial applications such as drilling in oil industry, generators, purification of industrial waste water and fabrication of optical fibers with pressurized coating in high speed drawing. The stability of Taylor-Couette flow has been the subject of numerous analytical and experimental investigations. Ostilla-Monico et al. [1] and Viazzo and Poncet [2] investigated turbulent Taylor-Couette flow by direct numerical simulation. They reported when there is a strong competition between an azimuthal flow induced by rotation and an axial flow due to convection; three different transition flow patterns are appeared. These patterns are either as spiral rolls, wavy vortices or a combination of both depending on the Taylor and Rayleigh numbers. Martinez-Arias et al. [3] and Ravelet et al. [4] experimentally determined the scaling of the torque with Reynolds numbers and the behaviour of the wall shear stress. At relatively high Reynolds number, a change in behaviour is observed corresponding to intersections of the torque–speed curves for different states. Weisberg et al. [5] also provided a test rig and determined the marginal stability diagram for the Taylor-Couette flow with periodic axial motion of the inner cylinder by using flow visualization. They concluded the enhanced stability is resulted because the Taylor-Couette flow requires a greater change in the azimuthal vorticity with axial motion of the inner cylinder. Using energy gradient theory is another procedure used to study the Taylor-Couette flow instability. In this regard, it is claimed that the energy gradient is possibly fairly universal for analysis of flow instability and turbulent transition, and is found valid for both pressure and shear driven flows in parallel and rotating flow, [6-8]. While a radial flow through the permeable walls of the cylinders is present, radial inflow and outflow have significant effect on Taylor vortex flow and wavy vortex flow. A small radial outflow velocity enhances the strength of the Taylor vortices resulting in destabilization of the base flow, whereas strong radial outflow and radial inflow reduce vortex strength, thus stabilizing the system. The transition to wavy vortex flow is unaffected by small radial outflow, but is stabilized for radial inflow, [9-11]. Meseguer and Marques [12,13] examined a comprehensive study of the linear stability on Spiral Couette solenoidal and Spiral Poiseuille flows. They accomplished the spatial discretisation of problem by a Petrov-Galerkin scheme. They found the zeroth order discontinuities on the neutral surface of stability in Spiral Couette and Spiral Poiseuille flows attributed to competition between two independent centrifugal and shear instabilities. Ali [14] studied stability analysis of Couette flow with axial movement of inner cylinder and determined neutral stability curve by shooting method, while Lee [15] applied the variational method to investigate the hydrodynamic stability for the motion of a viscous incompressible fluid between two coaxial cylinders which moved spirally along their common axis with assumption of small gap between the cylinders. Chang et al. [16] conducted an analysis for the linear stability of ferrofluid flow between two concentric rotating cylinders with a uniform axial magnetic field. Their results demonstrated that the applied axial magnetic field had a stabilizing effect for all conditions. They also showed increasing the gap between two cylinders will cause increasing the stability of the flow especially when both cylinders are counter-rotating. Chang et al. [17] also analyzed the stability of viscous flow between two infinitely long concentric rotating cylinders with an axial flow due to an axial pressure gradient by a direct numerical procedure. Hajmohammadi and Nourazar [18] employed two semi

analytical algorithms, differential transform and Adomian decomposition methods and Singh and Bajaj [19] used the Floquet's analysis to investigate the Taylor–Couette ferrofluid flow excited by a periodically oscillating magnetic field.

This paper has studied the stability analysis of the spiral Couette flow between two infinitely concentric cylinders. The Chebyshev tau method procedure has been developed by using Galerkin method and the orthogonality of Chebyshev polynomials. A complete linear stability analysis is implemented, in which three-dimensional disturbances including axisymmetric and non-axisymmetric modes are considered. Moreover, the Reynolds number is increased up to Re=2000 and is larger than 1350 which was used before by Meseguer and Marques [12, 20] and Ali [14].

II. GOVERNING EQUATIONS

First, in this study, we consider a viscous incompressible laminar flow between two concentric cylinders in which the outer cylinder is stationary and the inner one is rotating with axial motion, (Fig.1). The corresponding transient governing equations for continuity and momentums are as follows.

$$\frac{\partial u_z}{\partial z} + \frac{1}{r}\frac{\partial\, ru_r}{\partial r} + \frac{1}{r}\frac{\partial u_\phi}{\partial \phi} = 0 \tag{1}$$

$$\frac{\partial u_r}{\partial t} + u_r\frac{\partial u_r}{\partial r} + u_\phi\frac{\partial u_r}{r\,\partial \phi} + u_z\frac{\partial u_r}{\partial z} - \frac{u_\phi^2}{r} = -\frac{1}{\rho}\frac{\partial p}{\partial r} +$$
$$\nu\left[\nabla^2 u_r - \frac{u_r}{r^2} - \frac{2}{r^2}\frac{\partial u_\phi}{\partial \phi}\right] \tag{2}$$

$$\frac{\partial u_\phi}{\partial t} + u_r\frac{\partial u_\phi}{\partial r} + u_\phi\frac{\partial u_\phi}{r\,\partial \phi} + u_z\frac{\partial u_\phi}{\partial z} + \frac{u_r u_\phi}{r} =$$
$$-\frac{1}{\rho}\frac{\partial p}{r\,\partial \phi} + \nu\left[\nabla^2 u_\phi - \frac{u_\phi}{r^2} + \frac{2}{r^2}\frac{\partial u_r}{\partial \phi}\right] \tag{3}$$

$$\frac{\partial u_z}{\partial t} + u_r\frac{\partial u_z}{\partial r} + u_\phi\frac{\partial u_z}{r\,\partial \phi} + u_z\frac{\partial u_z}{\partial z} = -\frac{1}{\rho}\frac{\partial p}{\partial z} + \nu\nabla^2 u_z \tag{4}$$

u_r, u_ϕ, u_z are velocity components in the r, ϕ, z direction respectively. ν is kinetic viscosity, p is pressure and ρ is fluid density. With the assumptions of axial symmetry, $\partial(\ )/\partial\phi = 0$, fully developed flow, $\partial(\ )/\partial z = 0$, without axial pressure gradient and under the following boundary conditions, we have

$$\begin{aligned}
&\overline{u}_r(r_i,\phi,z) = 0, && \overline{u}_r(r_o,\phi,z) = 0 \\
&\overline{u}_\phi(r_i,\phi,z) = r_i\omega_i = u_{\phi i}, && \overline{u}_\phi(r_o,\phi,z) = 0 \\
&\overline{u}_z(r_i,\phi,z) = u_{zi}, && \overline{u}_z(r_o,\phi,z) = 0
\end{aligned} \tag{5}$$

The steady state solution of (1-4) denoted by and is given as:

$$\overline{u}_r = 0, \qquad\qquad \overline{u}_\phi = u_{\phi i}\frac{r_o^2 - r^2}{r_o^2 - r_i^2}\frac{r_i}{r}$$

$$\overline{u}_z = u_{zi}\frac{\ln(r/r_o)}{\ln(r_i/r_o)}, \qquad \frac{\partial \overline{p}}{\partial r} = \frac{\rho \overline{u}_\phi^2}{r} \tag{6}$$

$u_{\phi i}$ and u_{zi} are the rotational and axial velocity components of the rotor respectively. r_i is the rotor radius and r_o denotes the stator inside radius.

To study the stability of this flow, we superimpose a general disturbance on the steady state solution, i.e., the instantaneous flow parameters is divided into two parts, a main flow part and an infinitesimal perturbed one as: $u_r = \overline{u}_r + u_r'$, $u_\phi = \overline{u}_\phi + u_\phi'$, $u_z = \overline{u}_z + u_z'$, and $p = \overline{p} + p'$. The barred parameters indicate the steady state quantities and the parameters with prime sign ('') indicate unsteady perturbed quantities. Both the steady and the instantaneous flows satisfy the momentum equations. The steady and the instantaneous flow parameters are substituted separately into (1-4) and then their results are subtracted from each other. Subsequently, the result of the subtraction is expanded and linearized by dropping products of u_r', u_ϕ', u_z', the final result reads

$$\frac{1}{r}\frac{\partial\, ru_r'}{\partial r} + \frac{1}{r}\frac{\partial u_\phi'}{\partial \phi} + \frac{\partial u_z'}{\partial z} = 0 \tag{7}$$

$$\frac{\partial u_r'}{\partial t} + \overline{u}_\phi\frac{\partial u_r'}{r\,\partial \phi} + \overline{u}_z\frac{\partial u_r'}{\partial z} - 2\frac{\overline{u}_\phi u_\phi'}{r} = -\frac{1}{\rho}\frac{\partial p'}{\partial r} +$$
$$\nu\left[\nabla^2 u_r' - \frac{u_r'}{r^2} - \frac{2}{r^2}\frac{\partial u_\phi'}{\partial \phi}\right] \tag{8}$$

$$\frac{\partial u_\phi'}{\partial t} + u_r'\frac{\partial \overline{u}_\phi}{\partial r} + \overline{u}_\phi\frac{\partial u_\phi'}{r\,\partial \phi} + \overline{u}_z\frac{\partial u_\phi'}{\partial z} + \frac{u_r'\overline{u}_\phi}{r} = -$$
$$\frac{1}{\rho}\frac{\partial p'}{r\,\partial \phi} + \nu\left[\nabla^2 u_\phi' - \frac{u_\phi'}{r^2} + \frac{2}{r^2}\frac{\partial u_r'}{\partial \phi}\right] \tag{9}$$

$$\frac{\partial u_z'}{\partial t} + u_r'\frac{\partial \overline{u}_z}{\partial r} + \overline{u}_\phi\frac{\partial u_z'}{r\,\partial \phi} + \overline{u}_z\frac{\partial u_z'}{\partial z} = -\frac{1}{\rho}\frac{\partial p'}{\partial z} + \nu\nabla^2 u_z' \tag{10}$$

The above relations (7-10) are a linear system of equations for u_r', u_ϕ', u_z' and p' when the specified main flow $\overline{u}_r, \overline{u}_\phi, \overline{u}_z$ and $\overline{p}$ are given. Since (7-10) are linear for a small disturbance; it is natural to propose that a disturbance can be decomposed into normal modes of various wavelengths. A normal mode disturbance is a traveling wave with amplitude that depends on r-coordinate. Because the undisturbed flow quantities only depend on the r-coordinate, these disturbances can have the form

$$u'_j = \hat{u}_j(r)\exp[i(m\phi + kz + st)], \qquad j = r, \phi, z$$

$$p' = \hat{p}(r)\exp[i(m\phi + kz + st)] \qquad (11)$$

Here $\hat{u}_j(r)$ and $\hat{p}(r)$ are complex amplitude functions. i is the imaginary number, m is a real mode number in the $\phi-$ direction, and k is a real wave number in the $z-$ directions. s is a complex wave speed. The real part of gives the phase velocity of the wave, while the imaginary part of s reflects the growth rate of the disturbance. For the stability question, the most important quantity is the sign of the imaginary part of s. The growth or decay of (11) occurs if the imaginary part of s is negative or positive number respectively.

Introducing the main and perturbed velocity components from (6) and (11) into (7-10), yields the following dimensionless equations.

$$\left[\frac{d}{dr} + \frac{1}{r}\right]\hat{u}_r + i\left[\frac{m}{r}\hat{u}_\phi + k\hat{u}_z\right] = 0 \qquad (12)$$

$$\left\{ i\left[s + \frac{mu_{\phi i}r_i}{r_o^2 - r_i^2}\frac{r_o^2 - r^2}{r^2} + ku_{zi}\frac{Ln\,r/r_o}{Ln\,r_i/r_o}\right] \right.$$
$$\left. + \nu\left[\frac{1+m^2}{r^2} + k^2 - \frac{d}{rdr}(r\frac{d}{dr})\right] \right\}\hat{u}_r +$$

$$\left[i\frac{2m\nu}{r^2} - \frac{2u_{\phi i}r_i}{r_o^2 - r_i^2}\frac{r_o^2 - r^2}{r^2}\right]\hat{u}_\phi + \frac{1}{\rho}\frac{d\hat{P}}{dr} = 0 \qquad (13)$$

$$+\left\{ i\left[s + \frac{mu_{\phi i}r_i}{r_o^2 - r_i^2}\frac{r_o^2 - r^2}{r^2} + ku_{zi}\frac{Ln\,r/r_o}{Ln\,r_i/r_o}\right] \right.$$
$$\left. + \nu\left[\frac{1+m^2}{r^2} + k^2 - \frac{d}{rdr}(r\frac{d}{dr})\right] \right\}\hat{u}_\phi -$$

$$\left[i\frac{2\nu m}{r^2} + \frac{2u_{\phi i}r_i}{r_o^2 - r_i^2}\right]\hat{u}_r + i\frac{m}{\rho r}\hat{P} = 0 \qquad (14)$$

$$\left\{ i\left[s + \frac{mu_{\phi i}r_i}{r_o^2 - r_i^2}\frac{r_o^2 - r^2}{r^2} + ku_{zi}\frac{Lnr/r_o}{Lnr_i/r_o}\right] \right.$$
$$\left. + \nu\left[\frac{m^2}{r^2} + k^2 - \frac{d}{rdr}(r\frac{d}{dr})\right] \right\}\hat{u}_z +$$

$$\left[\frac{u_{zi}}{rLn\,r_i/r_o}\right]\hat{u}_r + i\frac{k}{\rho}\hat{P} = 0 \qquad (15)$$

For simplicity, we define the following parameters

$$r^* = \frac{r}{r_o}, \qquad \eta = \frac{2r^* - 1 - r_i^*}{1 - r_i^*}, \qquad s^* = \frac{s(r_o - r_i)^2}{\nu}$$

$$\frac{d}{dr} = \frac{2}{r_o - r_i}\frac{d}{d\eta} = \frac{2}{r_o - r_i}D, \qquad k^* = k(r_o - r_i)$$

$$Ta = \frac{4u_{\phi i}^2(r_o - r_i)^4}{\nu^2(r_o^2 - r_i^2)}, \qquad Re = \frac{(r_o - r_i)\hat{u}_{zi}}{\nu} \qquad (16a)$$

$$g = i\frac{2m(1 - r_i^*)^2}{r^{*2}} + r_i^*\sqrt{\frac{Ta}{1 - r_i^{*2}}}$$

$$f = i\left[\frac{mr_i^*}{2}\frac{1 - r^{*2}}{r^{*2}}\sqrt{\frac{Ta}{1 - r_i^{*2}}} + k^* Re\frac{Lnr^*}{Lnr_i^*}\right] +$$
$$\frac{(1 - r_i^*)^2}{r^{*2}}(1 + m^2) + k^{*2} \qquad (16b)$$

The dimensionless of (12-15) through the above parameters yields

$$\left[D + \frac{1 - r_i^*}{2r^*}\right]\hat{u}_r + i\left[\frac{m(1 - r_i^*)}{2r^*}\hat{u}_\phi + \frac{k^*}{2}\hat{u}_z\right] = 0$$

$$\left[is^* + f - \frac{2(1 - r_i^*)}{r^*}D - 4D^2\right]\hat{u}_r + \frac{2(r_o - r_i)}{\mu}D\hat{p} +$$
$$\left[g - \frac{r_i^*}{r^{*2}}\sqrt{\frac{Ta}{1 - r_i^{*2}}}\right]\hat{u}_\phi = 0 \qquad (17)$$

$$-g\hat{u}_r + \left[is^* + f - \frac{2(1 - r_i^*)}{r^*}D - 4D^2\right]\hat{u}_\phi +$$
$$i\frac{m(r_o - r_i)(1 - r_i^*)}{\mu r^*}\hat{p} = 0 \qquad (18)$$

$$\left[is^* + f - \frac{(1 - r_i^*)^2}{r^{*2}} - \frac{2(1 - r_i^*)}{r^*}D - 4D^2\right]\hat{u}_z +$$
$$\frac{Re(1 - r_i^*)}{r^* Lnr_i^*}\hat{u}_r + i\frac{k^*(r_o - r_i)}{\mu}\hat{p} = 0 \qquad (19)$$

$$\left[is^* + f - \frac{(1 - r_i^*)^2}{r^{*2}} - \frac{2(1 - r_i^*)}{r^*}D - 4D^2\right]\hat{u}_z +$$
$$i\frac{k^*(r_o - r_i)}{\mu}\hat{p} + \frac{Re(1 - r_i^*)}{r^* Lnr_i^*}\hat{u}_r = 0 \qquad (20)$$

Now, we obtain a relation between $\hat{u}_r$ and $\hat{u}_\phi$ by eliminating $\tilde{u}_z$ and $\hat{p}$ among (17), (19) and (20) with assumption of $r_i^* \to 1$ for simplicity. The final result after substituting is

$$\left[16D^4 - 4(f + k^{*2})D^2 + f\,k^{*2}\right]\hat{u}_r +$$

$$\frac{r_i^*}{r^{*2}}\sqrt{\frac{Ta}{1 - r_i^{*2}}}\,\hat{u}_\phi - is^*\hat{u}_r = 0 \qquad (21)$$

f is simplified by

$$f = i\left[\begin{array}{l} 0.5mr_i^*(1/r^{*2} - 1)\sqrt{Ta/(1 - r_i^{*2})}\ + \\ k^*\operatorname{Re} Lnr^* / Lnr_i^* \end{array}\right] + k^{*2}.$$

In a similar manner, by eliminating between (18) and (19) we have

$$4D^2 - f\ \hat{u}_\phi + g\hat{u}_r - is^*\hat{u}_\phi = 0 \qquad (22)$$

The required boundary conditions are:

$$\hat{u}_r(\eta = \pm 1) = 0, \qquad \hat{u}_\phi(\eta = \pm 1) = 0 \qquad (23)$$

The other two required boundary conditions based on (17) are

$$D\hat{u}_r(\eta = \pm 1) = 0 \qquad (24)$$

III. SOLUTION METHOLOGY

There are several methods to obtain the eigenvalues of the above set of homogeneous ordinary differential equations. In compound matrix method as discussed by Yiantsios and Higgins [21], the overall picture of the eigenvalue spectrum is not provided. The other method is shooting method. In this method we need a good guess of the eigenvalue and only a single eigenvalue is tracked. Another technique is finite difference approximations with non-convenient property that it converges slowly. The fourth technique is Chebyshev collocation method and we will now discuss it in detail, Canuto et al. [22]. This method takes away the aforementioned difficulties and unlike the finite difference technique has the convenient property that it converges exponentially.

The Chebyshev polynomials are eigenfunctions of the singular Sturm-Liouville problem consist of a family of orthogonal functions with weight function $1/\sqrt{1 - \eta^2}$ in the interval of $\eta \in [-1, 1]$. To approximate the eigenfunctions of the velocity components by truncated Chebyshev equations, we assume

$$\hat{u}_r = \sum_{n=0}^{N_r + h_r} a_n T_n(\eta) \qquad (25)$$

$$\hat{u}_\phi = \sum_{n=0}^{N_\phi + h_\phi} b_n T_n(\eta) \qquad (26)$$

In which, $T_n(\eta) = \cos(n\cos^{-1}\eta)$ is Chebyshev polynomial of the first kind, a_n and b_n are expansion coefficients and N

is number or degree of the polynomials. The optimum number of Chebyshev polynomials is calculated by trial and error technique. In this problem $h_r = 4$ and $h_\phi = 2$ denotes the order of differential equation, also, $h_r + h_\phi$ are the number of the boundary conditions of both equations $\hat{u}_r$ and $\hat{u}_\phi$. The derivative of expressions (25, 26) can be found by orthogonality conditions and recurrence relations used to arrive at expressions that do not contain derivatives of the Chebyshev polynomials as follows, Orszag [13].

$$\frac{d^{(q)}\hat{u}_r}{d\eta^4} = D^{(q)}\hat{u}_r = \sum_{n=0}^{N_r + h_r} a_n^{(q)} T_n(\eta) \qquad (27)$$

The recursion relation for a_n derivative of the coefficient is established as:

$$2na_n^{(q-1)} = d_{n-1}a_{n-1}^{(q)} - a_{n+1}^{(q)}, \quad n \geq 1, \quad if\ d_n = 1 + \delta_{0n} \qquad (28)$$

Substituting the expression (28) into (27), the relation between the Chebyshev coefficient a_n of $\hat{u}_r$ and the Chebyshev coefficient $a_n^{(q)}$ of $D^{(q)}\hat{u}_r$ is given by:

$$a_n^{(q)} = \Delta^q a_n \qquad (29)$$

$$\Delta = \begin{bmatrix} 0 & 1 & 0 & 3 & 0 & 5 & 0 & 7 & 0 & \dots & 0 \\ 0 & 0 & 4 & 0 & 8 & 0 & 12 & 0 & 16 & \dots & N \\ 0 & 0 & 0 & 6 & 0 & 10 & 0 & 14 & 0 & \dots & 0 \\ \dots & \dots & \dots & \dots & \dots & \dots & \dots & \dots & \dots & & \dots \\ 0 & 0 & 0 & 0 & 0 & 0 & 0 & 0 & 0 & \dots & N \\ 0 & 0 & 0 & 0 & 0 & 0 & 0 & 0 & 0 & \dots & 0 \end{bmatrix} \qquad (30a)$$

for even N

$$\Delta = \begin{bmatrix} 0 & 1 & 0 & 3 & 0 & 5 & 0 & 7 & 0 & \dots & \dfrac{N}{2} \\ 0 & 0 & 4 & 0 & 8 & 0 & 12 & 0 & 16 & \dots & 0 \\ 0 & 0 & 0 & 6 & 0 & 10 & 0 & 14 & 0 & \dots & N \\ \dots & \dots & \dots & \dots & \dots & \dots & \dots & \dots & \dots & & \dots \\ 0 & 0 & 0 & 0 & 0 & 0 & 0 & 0 & 0 & \dots & N \\ 0 & 0 & 0 & 0 & 0 & 0 & 0 & 0 & 0 & \dots & 0 \end{bmatrix} \qquad (30b)$$

for odd N

This allows us to write (21, 22) in a matrix form as:

$$A \quad B \begin{bmatrix} 16\Delta^4 - 4(f + k^{*2})\Delta^2 + f\,k^{*2}\mathbf{I} & g\,\mathbf{I} \\[2mm] \dfrac{r_i^*}{r^{*2}}\sqrt{\dfrac{Ta}{1-r_i^{*2}}}\,\mathbf{I} & 4\Delta^2 - f\,\mathbf{I} \end{bmatrix} =$$

$$is^* \; A \quad B \begin{bmatrix} \mathbf{I} & 0 \\ 0 & \mathbf{I} \end{bmatrix} \qquad (31)$$

where $A \quad B = \begin{bmatrix} a_0, a_1, \dots a_{N_r+4} & b_0, b_1, \dots b_{N_\phi+2} \end{bmatrix}$.

Using (28), the first, second and fourth order derivatives are

$$a_n^{(1)} = \frac{2}{d_n} \sum_{\substack{k=n+1 \\ k+n \ \text{odd}}}^{N_r+4} k a_k, \qquad k \geq 0 \qquad (32a)$$

$$a_n^{(2)} = \frac{1}{d_n} \sum_{\substack{k=n+2 \\ k+n \ \text{even}}}^{N_r+4} k(k^2 - n^2) a_k, \qquad k \geq 0 \qquad (32b)$$

$$a_n^{(4)} = \frac{1}{24 d_n} \sum_{\substack{k=n+4 \\ k+n \ \text{even}}}^{N_r+4} k \begin{bmatrix} k^2(k^2-4)^2 - 3k^4 n^2 + \\ 3k^2 n^4 - n^2(n^2-4)^2 \end{bmatrix} a_n \qquad (32c)$$

The number d_n being defined by $d_0 = 2$ and $d_n = 1$ for $n \geq 1$. In a similar manner, the derivatives of $D^{(q)}\hat{u}_\phi$ and $b_n^{(q)}$ can be derived.

We collocate the approximations (25, 26) at the Gauss-Lobatto grid [22] points as:

$$\eta_j = \cos\frac{j\pi}{N}, \qquad j = 0,1,2,\dots N \qquad (33)$$

These grid points give $(N_r + 1) + (N_\phi + 1)$ equations for the expansion coefficients of $(a_0, a_1, \dots a_{N_r})$ and $(b_0, b_1, \dots b_{N_\phi})$, whereas in total there are $\sum_{j=r,\phi} N_j + h_j + 2$ unknowns. The remaining unknown expansion coefficients, i.e., $a_{N_r+1}, a_{N_r+2}, \dots a_{N_r+4}$ and $b_{N_\phi+1}, b_{N_\phi+2}$ are obtained from the boundary conditions. Substituting expressions (25, 26) into the boundary conditions (23, 24) and bearing in mind $T_n(\pm1) = (\pm1)^n$ and $T'_n(\pm1) = (\pm1)^{n+1} n^2$, these results are

$$\sum_{i=1}^{N_r+4} (\pm1)^n a_{N_r+i} = 0 \qquad (34a)$$

$$\sum_{i=1}^{N_r+4} (\pm1)^{n+1} n^2 a_{N_r+i} = 0 \qquad (34b)$$

$$\sum_{i=1}^{N_\phi+2} (\pm1)^n b_{N_\phi+i} = 0 \qquad (34c)$$

To improve the solution, let us first assume (21, 22) are defined as $L_1(\hat{u}_r, \hat{u}_\phi) = 0$ and $L_2(\hat{u}_r, \hat{u}_\phi) = 0$ respectively, in which is differential operator. Due to a truncation of the $N + h\,th$ Chebyshev polynomial of an infinite expansion, the tau method argues that rather than solving equation of $L_i(\hat{u}_r, \hat{u}_\phi) = 0, i = 1, 2$ one instead solves the following equation.

$$L_i(\hat{u}_r, \hat{u}_\phi) = \sum_{j=1}^{h} \tau_{i,j} T_{N+j}(\eta) \quad \begin{array}{ll} i = 1 & j = 1,2,3,4 (= h) \\ i = 2 & j = 1,2 (= h) \end{array} \qquad (35)$$

Where $\tau_{i,j}$ are tau coefficients which may be used to measure the error associated with the truncation of $L_i(\hat{u}_r, \hat{u}_\phi) = 0, \ i = 1, 2$. These unknown $\tau_{i,j}$ coefficients can be computed from the following equation by making use of the orthogolality of the functions $T_{N+i}\ \eta$ in the interval $\eta \in [-1,\ 1]$ as:

$$\int_{-1}^{1} \frac{T_{N+j}(\eta) . L_i(\hat{u}_r, \hat{u}_\phi)}{\sqrt{1-\eta^2}} d\eta = \int_{-1}^{1} \frac{T_{N+j}(\eta) . \sum_{j=1} \tau_{i,j} T_{N+j}(\eta)}{\sqrt{1-\eta^2}} d\eta =$$

$$\tau_{i,j}\, \|T_{N+j}\|^2 \qquad (36)$$

$$\begin{array}{ll} i = 1, & j = 1,2,3,4 \\ i = 2, & j = 1,2 \end{array}$$

$\|T_{N+i}\| = \pi / c_i$ is associated norm and $c_i = 0$, if $i \neq N + i$ or $c_j = 2$, if $i = N + i$.

The system of equations where includes (31), (34a, 34b) and (35) are homogeneous, linear in a_n, b_n and contain the eigenvalue s^*, allows us to write the system of equations as a generalized eigenvalues problem as:

$$X \quad P = s^* X \quad Q \qquad (37)$$

wher s^* and $\mathbf{X}$ are eigenvalues and eigenvectors respectively.

The Q matrix is inevitably singular due to the way the boundary conditions rows are added to P. However, from boundary conditions, we can easily eliminate the $a_{N_r+i}, i = 1, 2, 3, 4$ and $b_{N_\phi+i}, i = 1, 2$. Thus the $a_{N_r+i}, i = 1, 2, 3, 4$ and $b_{N_\phi+i}, i = 1, 2$ rows of matrix P may be removed and the $N_r + i,\ i = 1, 2, 3, 4$ and $N_\phi + i,\ i = 1, 2$ columns eliminated using (34a, 34b). This yields $(N+1) \times (N+1)$ matrix P and the matrix problem which results from (37) does not suffer from being singular due to zero boundary condition rows.

After combing s. (31, 34a, 34b), the final result in a matrix form is as flows

$$A \quad B \quad \times$$

$$\begin{bmatrix} C\mathbf{I} & g\mathbf{I} & M_1 & M_2 & 0 & 0 & M_5 & M_6 \\ D\mathbf{I} & E\mathbf{I} & 0 & 0 & M_3 & M_4 & 0 & 0 \end{bmatrix} =$$

$$is^* \quad A \quad B \begin{bmatrix} \mathbf{I} & 0 & 0 & 0 & 0 & 0 & 0 & 0 \\ 0 & \mathbf{I} & 0 & 0 & 0 & 0 & 0 & 0 \end{bmatrix} \qquad (38)$$

where,

$$C = 16\Delta^4 - 4(f + k^{*2})\Delta^2 + f\, k^{*2}$$

$$D = \frac{r_i^*}{r^{*2}}\sqrt{\frac{Ta}{1 - r_i^{*2}}}, \qquad E = 4\Delta^2 - f$$

In which

$$\mathbf{A}\underbrace{1,\,1,\,\ldots}_{\mathbf{M_1}}{}^T = \mathbf{0}, \qquad A\underbrace{\left[1,\,-1,\,\ldots(-1)^{N+4}\right]}_{M_2}{}^T = \mathbf{0} \qquad (39a)$$

$$B\underbrace{1,\,1,\,\ldots}_{M_3}{}^T = \mathbf{0}, \qquad B\underbrace{\left[1,\,-1,\,\ldots(-1)^{N+4}\right]}_{M_4}{}^T = \mathbf{0} \qquad (39b)$$

$$A\underbrace{\left[1,\,1,\,\ldots(N+4)^2\right]}_{M_5}{}^T = \mathbf{0}, \qquad (39c)$$

$$A\underbrace{\left[0,\,1,\,\ldots(-1)^{N+4}(N+4)^2\right]}_{M_6}{}^T = \mathbf{0} \qquad (39d)$$

IV. RESULTS AND DISCUSSION

The stability of basic flow is determined by the sign of the imaginary part of the eigenvalues of (38). If $Imag(s^*) > 0$, the flow is stable and if $Imag(s^*) < 0$, the flow is unstable.

Table 1 shows the critical Taylor number and wavelength corresponding to four different Chebyshev polynomial numbers at $Re=0$. The Taylor number corresponding to the threshold of the instability is called the critical Taylor number. It is seen that having 25 polynomials is good enough to calculate the critical Taylor number accurately. This number of polynomials will be applied for the other cases. Fig. 1 illustrates the critical Taylor number versus Reynolds number in axisymmetric condition i.e., at $m=0$. As seen, the axial velocity stabilizes the spiral Couette flow in the axisymmetric mode. In the other words, increasing the axial velocity increases the critical Taylor number. Also, comparison between the present results and the data of Ali [14] exhibits a good agreement between them. The main source of instability is the Taylor cells generated in the gap between two cylinders.

TABLE I. CRITICAL TAYLOR NUMBER AND WAVELENGTH FOR DIFFERENT CHEBYSHEV POLYNOMIAL NUMBERS AT $RE=0$

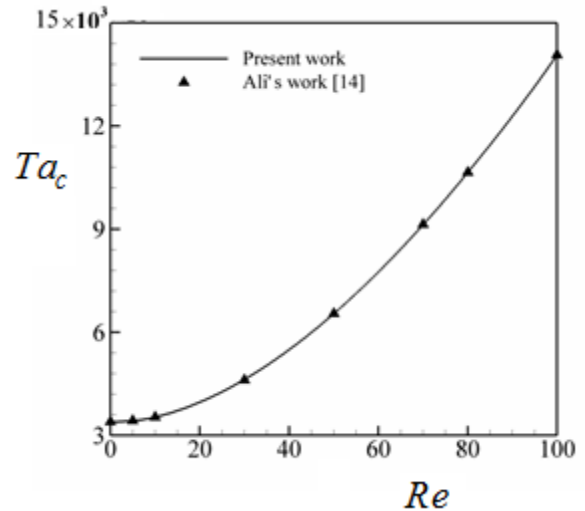| polynomial numbers	Ta_c	λ_c
10	3389.771875	3.1266
15	3389.900386	3.1266
25	3389.900267	3.1265
35	3389.900267	3.1265

Figure 1. Critical Taylor number versus Reynolds number at m=0

Table 2 reproduces Fig. 1 for three flow characteristics including the critical Taylor number, wave number and frequency for different Reynolds numbers in the range of $0 \le Re \le 2000$. The results indicate that the axial velocity on the rotating cylinder (inner one) reduces the instability. The reason is that this flow condition approaches the planar Couette flow which is unconditionally stable. Since the axial velocity increases by increasing Reynolds number and sweeps the fluid element, the Taylor cell is elongated under the most unstable mode. So, the wavelength will be enhanced by Reynolds number. On other hand, the critical frequency is increased and the flow characteristic is transferred faster from one point to another one in the fluid.

TABLE II.   CRITICAL TAYLOR NUMBER, WAVE NUMBER AND FREQUENCY FOR DIFFERENT REYNOLDS NUMBERS AT $m=0$

Re	Ta_c	k_c^*	s_c^*
0	*3389.90*	3.1265	0
5	3425.60	3.1151	8.1975
10	3531.97	3.0807	16.2272
50	6540.05	2.5113	67.2544
80	10647.94	2.1636	93.8205
100	14068.06	1.9894	108.4286
200	38743.47	1.4356	158.0927
500	190546.67	0.7890	217.7599
1000	715765.60	0.4413	243.9145
1500	1587879.52	0.3032	251.4338
2000	2808211.69	0.2300	254.4141

Fig. 2 illustrates the critical Taylor number as a function of the mode number, m, for different Reynolds numbers. The ordinate axis has been normalized by the critical Taylor number at m=0. The mode number zero, i.e., m=0 is corresponding to the axisymmetric mode. The results state that $Ta_c / Ta_c (m=0) > 1$ for all mode numbers. It means that the process is more stable for non-axisymmetric mode especially for large mode numbers at high Reynolds number.
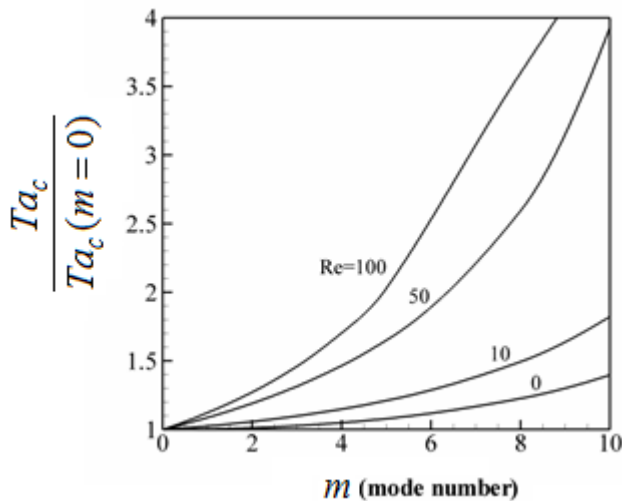
Figure 2.   Critical Taylor number versus mode number for different Reynolds numbers

Fig. 3 reports the critical period time of a perturbed flow against mode number. The findings show the critical period time at *Re=0* has the largest value at any mode number. In the other words, the higher critical period time the more unstable situation will be occurred. The reason is that the perturbed flow propagates more in the flow and causes more instability. This instability is more sever at low mode numbers especially at low

Reynolds numbers. Furthermore, the critical period time at *Re=0* and *m=0* is infinity, so the perturbed flow has enough time to propagate throughout the fluid domain. Since *m=0* is corresponding to the axisymmetric situation, hence the flow is most unstable.
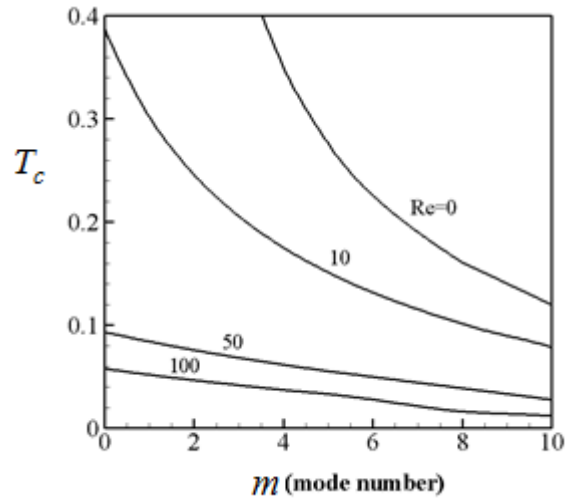

Figure 3.   Critical period time versus mode number for different Reynolds numbers

Figs 4 (a-d) present the real part of the critical eigenmodes of flow characteristics for different mode numbers at *Re=50*. Fig. (4c) shows the $\tilde{u}_{zc}$ components of axisymmetric eigenmode is zero at $(r - r_i)/(r_o - r_i) \simeq 0.38$, while this point is converted to two points, $(r - r_i)/(r_o - r_i) \simeq 0.34$ and $(r - r_i)/(r_o - r_i) \simeq 0.75$ for more stable nonaxisymmetric mode at *m=1*. There is a stationary point at $(r - r_i)/(r_o - r_i) \simeq 0.46$ for the nonaxisymmetric mode at *m=2* where the velocity magnitude is zero. This trend continues for *m=4* and *m=10* with more points including zero velocity components and it can be concluded the zero velocity points increases for more stable non-axisymmetric modes. It seems that the exponential behaviour of $Ta_c / Ta_c (m=0)$ is also generated by these zero points.
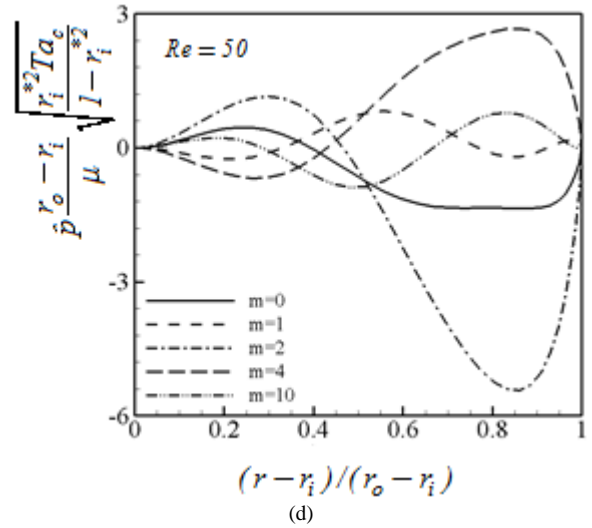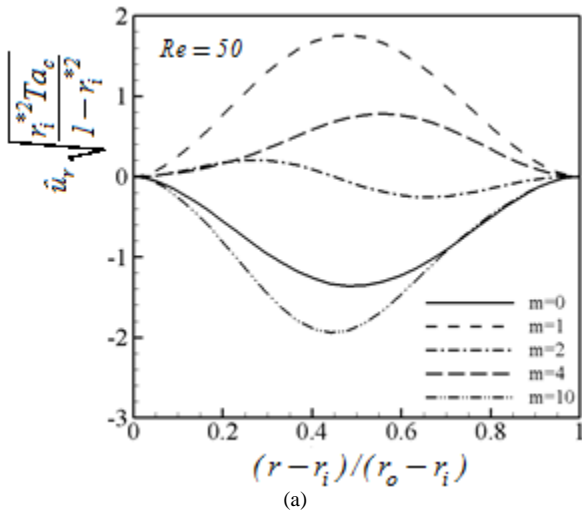
(a)

(b)

(c)

(d)

Figure 4. (a-d) Real parts of critical eigenvectors of flow characteristics for different mode numbers at *Re=50*
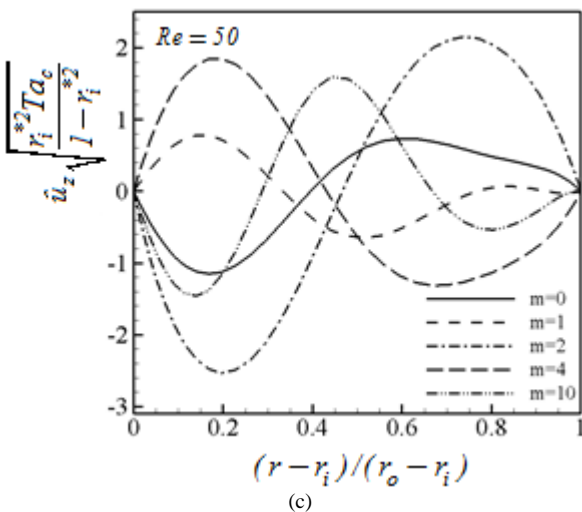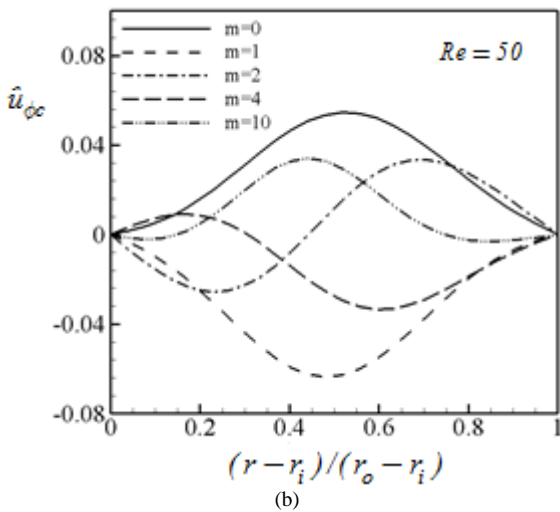
Fig. 5 shows the perturbed stream lines in the gap region at *Re=50* and *m=0* for four wavelengths. The corresponding critical wave number is $\lambda_c = 2.5113$. λ is a wavelength and measures a longitude distance for a single vortex. It should be noted that the direction of velocity at each vortex changes from one center to another one and after two more vortex repeats itself again. This wavy behavior is just similar to the streamlines reported by Hwang and Yang [23] for mean streamlines of and $Ta = 123$.
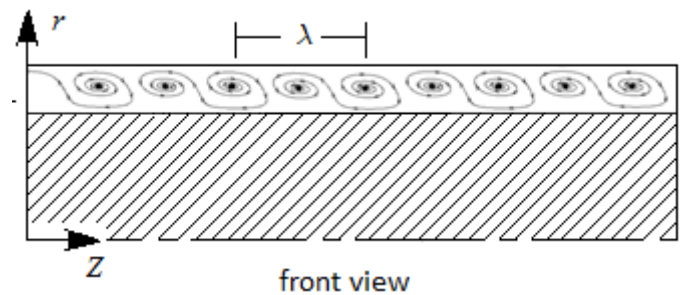
Figure 5. Critical streamlines at *Re=50* and *m=0*

Fig. 6 (a-c) depicts the real parts of the perturbed contour velocities, $\hat{u}_{rc} = \hat{u}_r \sqrt{r_i^{*2} Ta_c / (1 - r_i^{*2})}$, $\hat{u}_{\phi c} = \hat{u}_\phi \big|_{Ta_c}$ and $\hat{u}_{zc} = \hat{u}_z \sqrt{r_i^{*2} Ta_c / (1 - r_i^{*2})}$ in the same computational domain of the previous plot. As seen, the contours of $\hat{u}_{\phi c}$ and $\hat{u}_{zc}$ are almost in the same phase but the real part of $\tilde{u}_{rc}$ has a delay about $\pi / 2$ radians respect to the others. In addition, the locus of zero contours in Figs. (7a, 7b) are inclined respect to
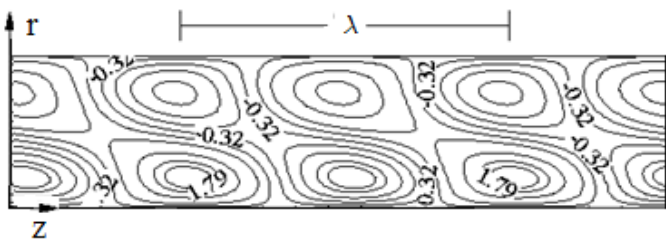
the mean velocity, while zero contours locus of $\hat{u}_{rc}$ are normal to the mean velocity vector.
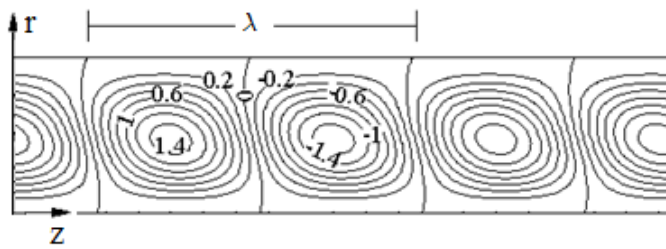
(a)-Real part of critical contours of $\hat{u}_{rc}$
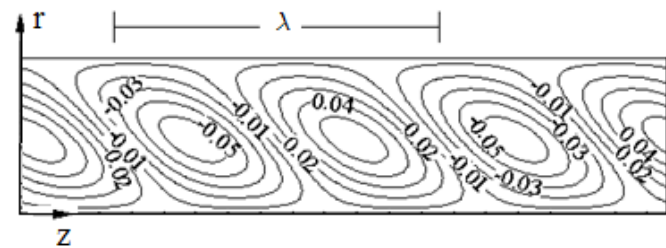
(b)- Real part of critical contours of $\hat{u}_{\phi c}$

(c)- Real part of critical contours of $\hat{u}_{zc}$

Figure 6. (a-c) Velocity eigenmodes at *Re=50* and *m=0*

Fig. 7 reproduces Fig. 5 but for non-axisymmetric modes at *Re=50* and *m=4*. The overall shape of perturbed vortexes is preserved in the r-z plane in comparison to the axisymmetric case. It is interesting to note that the streamlines in the $r-\phi$ plane is completely different from the axisymmetric mode and four loop shapes are generated in the half of cross section. The quantity of these loops are equal to the mode of instability and increasing of these loops with zero velocity boundary helps the flow to be more stable, while it does not take place in the symmetric case.
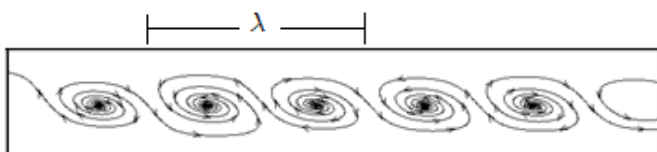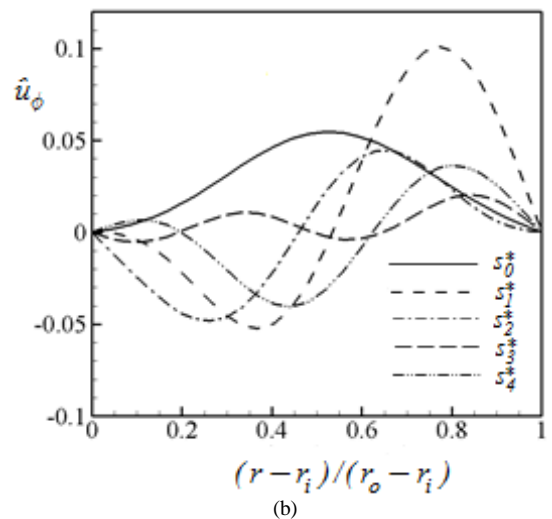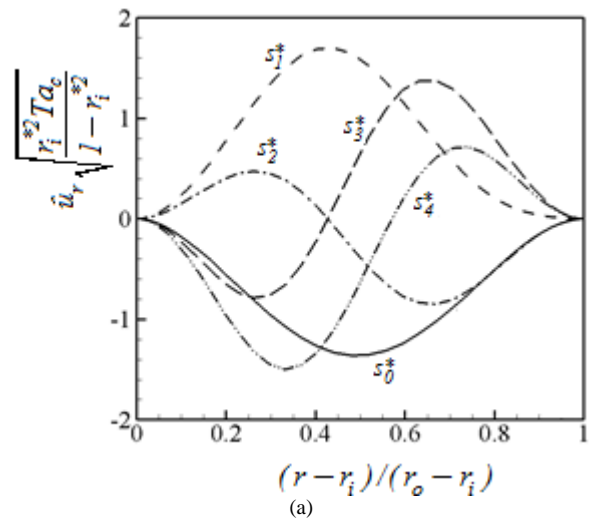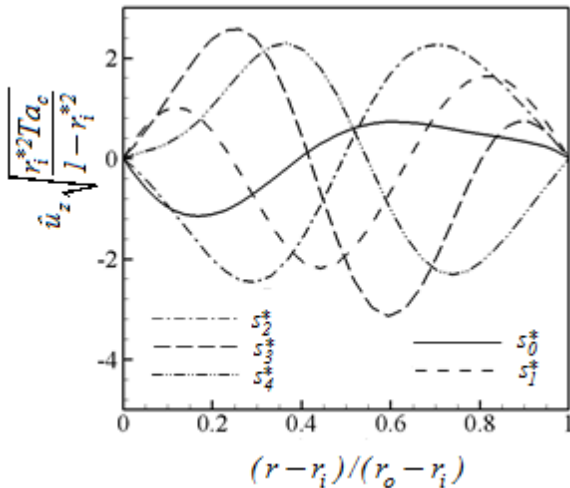

Figure 7. Critical non-axisymmetric streamline at *Re=50* and *m=4*

Fig. 8 (a-d) exhibit the eigenvectors of flow characteristics including velocity components as well as pressure for different eigenvalues at *Re=50* and *m=0*. The values of eigenvalues are

$$s_o^* = -67.25, \qquad s_1^* = -54.89 + 46.09\,i,$$

$$s_2^* = -63.98 + 57.85\,i, \qquad s_3^* = -66.51 + 91.88\,i \qquad \text{and}$$

$$s_4^* = -60.59 + 93.59\,i\,.$$ It is noted the imaginary part of s_o^* is zero because this mode belongs to the unstable condition. The behavior of these plots is more or less is similar to the previous plots. One can simply observe that curves with more zero velocity points belong to more stable conditions.
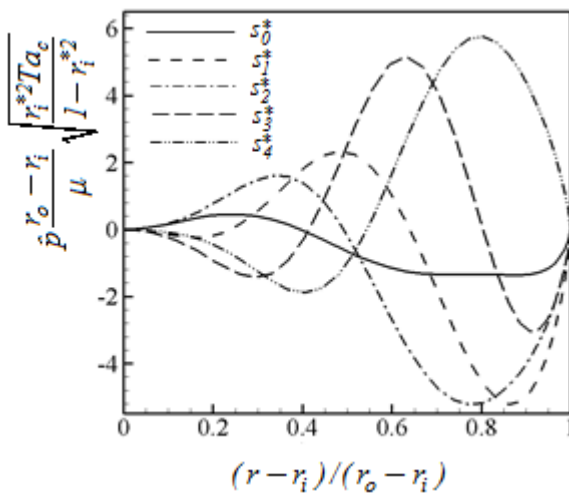

(a)

(b)

(c)

(d)

Figure 8. (a-d) Eigenvectors of flow characteristics for different eigenvalues at *Re=50* and *m=0*

V. CONCLUSIONS

The Chebyshev tau method is used to solve the stability equations of a spiral Couette flow between two coaxial cylinders with axial motion and rotating of the inner cylinder. The Chebyshev tau method is a powerful tool to solve linear eigenvalue equations. It is found that the axial motion leads to decay the centrifugal instability and causes more stable condition. In addition, the axial velocity increases the flow stability and the non-axisymmetric mode is more stable than the corresponding axisymmetric one for all Reynolds number. Also, the axisymmetric eigenvalue equations are more unstable than the non-axisymmetric and wavy patterns. In addition, the velocity eigenmodes with more zero velocity points are attributed to the more stable conditions.

REFERENCES

[1] R. Ostilla-Monico, E.P. Poel, R. Verzicco, S. Grossmann, and D. Lohse, "Boundary layer dynamics at the transition between classical and the ultimate regime of Taylor-Couette flow", Physics of Fluids, 26, 2014.

[2] S. Viazzo, and S. Poncet, S., "Numerical simulation of the flow stability in a high aspect ratio Taylor–Couette system submitted to a radial temperature gradient", Computer and Fluids, vol.101, No.20, 2014, pp.15-26.

[3] B.J. Martínez-Ariasa1, J. Peixinho, O. Crumeyrolle, and I. Mutabazi, "Effect of the number of vortices on the torque scaling in Taylor–Couette flow", J. of Fluid Mechanics, 748, 2014, pp.756-767.

[4] F. Ravelet, R. Delfos, and J. Westerweel, "Influence of global rotation and Reynolds number on the large-scale features of a turbulent Taylor–Couette flow", Physics of Fluids, Vol.22, No.5, 2010.

[5] A.Y. Weisberg, A. Smits, and I. Kevrekidis, "Delaying transition in Taylor-Couette flow with axial motion of the inner cylinder", J. of Fluid Mechanics, 348, 1997, pp. 141-151.

[6] R.K. Deka, and H.S. Takha, "Hydrodynamic stability of viscous flow between curved porous channel with radial flow", Int. J. of Engineering Science, Vol.42, No.10, 2004, pp 953-966.

[7] H.S. Dou, B.C. Khoo, and K.S. Yeo, "Instability of Taylor-Couette flow between concentric rotating cylinders", Int. J. Of Thermal Science, Vol.47, No. 11, 2008, pp. 1422-1435.

[8] M.A. Fardin, T.J Ober, C. Gay, G. Gregoire, G.H. McKinley, and S. Lerouge, "Criterion for purely elastic Taylor-Couette instability in the flows of shear-banding fluids", A Letters J. Exploring the Frontiers of Physics, Vol.96, No.4, 2011.

[9] S. Maretzke, B. Hof, B. and M. Avila, "Transient growth in linearly stable Taylor-Couette flows", J. of Fluid Mechanics, 742, 2014, pp.254-290.

[10] D. Martinand, E. Serre, and R.M. Lueptow, "Absolute and convective instability of cylindrical Couette flow with axial and radial flows", Physics of Fluids, 21, 2009.

[11] E. Serre, M.A. Sprague, and R.M. Lueptow, "Stability of Taylor-Couette flow in a finite-length cavity with radial throughflow", Physics of Fluids, 20, 2008.

[12] A. Meseguer, and F. Marques, "On the competition between centrifugal and shear instability in spiral Couette flow", J. of Fluid Mechanics 402, 2000, pp. 33-56.

[13] S.A. Orszag, "Accurate solution of the Orr-Sommerfield stability equation", J. of Fluid Mech. 50, 1971, p.689.

[14] M.A. Ali, "The stability of Couette flow with an inner cylinder rotating and moving with a constant axial velocity", Fluid Dynamics Research, 27, 2000, pp. 109-115.

[15] M.H. Lee, "The stability of spiral flow between coaxial cylinders", Computers & Mathematics with Application, Vol.41, No.3-4, 2001, pp. 289-300.

[16] M.H. Chang, C.K. Chen, and H.C. Weng, "Stability of ferrofluid flow between concentric rotating cylinders with an axial magnetic field", Int. J. of Engineering Science, 41, 2003, pp.103–121.

[17] M.H. Chang, and C.K. Chen, "The stability of the narrow-gap Taylor-Couette system with an axial flow", Acta Mechanica, 156, 2002, pp.131-143.

[18] M.R. Hajmohammadi, and S.S. Nourazar, "On the solution of characteristic value problems arising in linear stability analysis; semi analytical approach", Applied Mathematics and Computation, vol.35, No.15, 2014, pp.126-132.

[19] J. Singh, and R. Bajaj, "Parametric modulation in the Taylor–Couette ferrofluid flow", Fluid Dynamics Research, 40, 2008, pp. 737–752.

[20] A. Meseguer, and F. Marques, "Axial effects in the Taylor-Couette problem: Spiral-Couette and spiral-Poiseuille flows", Lecture Notes in Physics, 549, 2000, pp. 118-136.

[21] S.G. Yiantsios, and B.G. Higgins, "Numerical solution of eigenvalue problems using the compound matrix method", J. of Computational Physics, vol.74, No.1, 1998, pp.25-40.

[22] C. Canuto, M.Y. Hussaini, A. Quarteroni, and T.A. Zang, Spectral methods: Fundamentals in single domains, Springer-Verlag, Berlion Heidelberg, Germany, 2006.

[23] Hwang, Jong-Yeon, Yang, Kyung-Soo, 2004, "Numerical study of Taylor–Couette flow with an axial flow", Computers and Fluids, 33, 2004, pp.97-118.